<Original Article>

A NELL-1 Binding Protein: Vimentin

Hwa-Sung Chae[1,2,3], Young-Ho Kim[1]

1. Department of Orthodontics, The Institute of Oral Health Science, Samsung Medical Center, Sungkyunkwan University School of Medicine, Seoul, Korea
2. Department of Molecular Genetics, Seoul National University School of Dentistry, Seoul, Korea
3. Clinical Visiting Professor, Section of Orthodontics, School of Dentistry, University of California, Los Angeles, California, USA

Corresponding Author

Young-Ho Kim, DDS, MS, PhD
Department of Orthodontics, The Institute of Oral Health Science, Samsung Medical Center, 50 Irwon-dong, Gangnam-gu, Seoul 135-710, Korea
TEL : +82-2-3410-2425 FAX : +82-2-3410-0038 E-mail : huyyoung@skku.edu

Received for publication Feb 4, 2011; Returned after revision Apr 6, 2011;
Accepted for publication Apr 20, 2011

· Abstract

Purpose: Craniosynostosis (CS), one of the most common congenital craniofacial deformities, is the premature closure of cranial sutures. NELL-1 is a novel molecule overexpressed during premature cranial suture closure in human CS. From a functional perspective, NELL-1 has been reported to accelerate chondrocyte maturation and modulate calvarial osteoblast differentiation and apoptosis pathways. The mechanism through which NELL-1 induces these phenomena, however, remains unclear. The purpose of this study is to identify the NELL-1 binding protein(s) through which the biologic mechanism of NELL-1 can be further investigated.
Materials and Methods: Far-Western and Immunoprecipitation (IP) assays were performed, independently and in sequence, followed by mass spectrometry to identify the NELL-1 binding proteins. Reverse IP was used to verify and confirm candidate binding protein.
Results: The only confirmative protein from current experimentation was vimentin. Vimentin is the major structural component of the intermediate filaments.
Conclusion: The present study identified and confirmed vimentin as a NELL-1 binding protein, which opened up a new window to mechanistically facilitate studies on this CS-associated molecule.

· Key word : NELL-1 protein, Vimentin, Far-Western blotting, Mass spectrometry

· J Kor Dent Sci. 2011; 4(1) : 6 - 13

Introduction

Synostosis is defined as a union of two or more bones to form one bone. A synostotic event may occur anywhere ligaments closely approximate two or more bones, and once the ligament calcifies to form a bony union. Craniosynostosis (CS) stems from the premature closure of the cranial sutures and affects one in 2,500~3,000 persons[1,2]. Nel, is an abbreviation for *Neural tissue encoding Epidermal growth factor (EGF) Like domain* and is a secreted protein. Structurally, Nell-1 encodes a secretory signal peptide sequence, an NH2-terminal thrombospondin-1-like module, five Von Willebrand factor-like repeats with six cysteine residues, and six EGF-like domains[3]. Nell-1 is also highly conserved across species. For example, 93% amino acid sequence homology exists between rat Nell-1 and human NELL-1. Nell-1 encodes a polypeptide with a molecular weight of 90 kDa. When overexpressed in COS (Cells being CV-1 [Simian] in Origin) cells, the glycosylated form is N- linked to a 50 kDa carbohydrate moiety in eukaryotic cells to generate the 140 kDa form found in the cytoplasm. This 140 kDa protein is further processed to become a 130 kDa protein. The Nell-1 protein is secreted in trimeric form with a large molecular weight (approximately 400 kDa)[3]. Even though many studies have attempted to understand the molecular etiology of CS, the biological mechanisms of normal suture patency and premature closure remain largely unknown. Although NELL-1 has not yet been identified as a cause of CS in human genetic studies, NELL-1 may be a part of a complex chain of events resulting in premature suture closure because previous studies indicate that Nell-1 presents an exciting new protein with specific and significant osteochondral potential. Application of Nell-1 induced various bone formation processes gives promising results for further investigation. Potential clinical applications of NELL-1 include repair of facial clefts as well as in wound healing.

The discovery of the NELL-1 receptor is of clinical importance as once it is elucidated, the specific drug which targets the NELL-1 receptor and subsequently inhibits the transduction of its signal, may potentially resolve CS, reducing the probability of an inevitable surgery and any untoward side effects resulting from such an intervention. The specific molecular mechanism of NELL-1's role in CS is still under investigation. The objective of this research is to find the potential NELL-1 binding protein associated with the membrane portion of osteoblastic cells, which would provide an insight into the biologic mechanism of NELL-1 and its role in CS.

Materials and Methods

1. Cell culture and extraction of membrane protein

Using cell membrane extraction protocol[4], the membrane and cytosol protein portion was extracted from our cultured cells. $SAOS_2$ (human osteogenic sarcoma cell line), primary calvarial cells (fetal mouse osteoblast, extracted from 8 day old mice), and WI38 (human embryonic fibroblast, lung-derived cell line) were used for this study. Cells were grown in 10 cm^2 cell culture dishes until 80% confluent. 10 ml of differentiation media composed of 10 ml of complete Dulbecco's Modified Eagle Medium, 50 µl ascorbic Acid, 100 µl b-GP (1 M), 1 µl DEX (10^{-4}M) were added, and cells were harvested at 48 hours. For harvesting cells, the media was removed and washed twice with cold 1× PBS, followed by 0.3 ml of 10 mM Tris at pH 7.4. For immunoprecipitation, 1% NP40 was added to remove the proteins extracted in mild non-ionic detergent. Cells were collected using lifter and frozen in 1.5 ml microfuge tubes. Cells were then thawed and centrifuged at 12,000 rpm for 30 min. The supernatant, containing cytosolic proteins, was separated and saved, and the pellet was resuspended and incubated at 4ºC for two hours in RIPA buffer (Pierce #89900, IL, USA: 25 ml Tris-HCl pH 7.6, 150 mM NaCl, 1% NP 40, 1% Sodium deoxycholate, 0.1% SDS) with one tablet of protease inhibitor (Roche Catalog #1836170, Basel, Switzeland) added per 1 ml of RIPA buffer to solubilize the cell membrane proteins. The microtubes were spun at 12,000 rpm for 30 min, and the supernatant containing the membrane proteins was collected. Fractions were analyzed for protein content by measuring the optical density (Bio-rad RC DC Protein Assay Reagents Package, CA, USA) at a wavelength of 750 nm.

2. Far-Western Assay

60 µg extracted proteins were mixed with 5× reducing and non-reducing sample buffers respectively and run on PAGE gel at a voltage of 100 V constantly for about one hour until the dye approximated the bottom of gel. Proteins were transferred to a nitrocellulose membrane which was blocked by protein-free (TBS) blocking buffer (Pierce, IL, USA #37570). The membrane was then incubated overnight at

4°C in PBS containing 12 ml of NELL-1-His (5 μg/ml). The membrane was then washed three times for 15 min in TBS–Tween 20 at room temperature (RT). The membrane was then incubated in 12 ml blocking buffer containing 1:5,000 HisProbe™-HRP (Pierce, IL, USA #15165) for one hour at RT. Next, the membrane was washed three times in TBS–Tween 20 at RT. Specific bands were visualized by incubating membranes in SuperSignal West Pico solution (Pierce, IL, USA #34079).

3. Immunoprecipitation and Far-Western Assay

TALON Metal Affinity Resin (Clontech, WI,USA #635504) was washed in 500 μl PBS 1× three times, and resuspended in 500 μl PBS solution. 40 μg of NELL-1-his was incubated in 40 μl of washed beads as described above and agitated for one hour at room temperature. The NELL-1-his bound resin was then washed three times in PBS 1× using a 27 gauge needle to remove all supernatant. The pellet was resuspended in 40 μl of PBS. 1 mg of the protein extracted from the membrane portion was added to each tube to pull down the antibody complex. Samples were incubated at 4°C overnight on a shaker. The immunocomplex was washed three times with 1× PBS. After the final wash, each pellet was resuspended in 2× sample buffer and a total of 40 μl of sample was resolved by electrophoresis and transferred to nitrocellulose and Far-Western blotting was performed as described above. Washed beads without NELL-1 were used as negative control.

4. In-gel Digestion, Mass Spectrometry, and Database search

Bands were identified in both Far-Western and immunoprecipitation followed by Far-Western. The gels were subsequently stained in Gelcode Blue Stain Reagent (Pierce, IL, USA #24590) and then destained according to the manufacturer instruction. Protein bands in the range of 75 kDa and 55 kDa were separated from the gel to be analyzed (Applied Biomics, CA, USA). The samples were digested in-gel with modified porcine trypsin protease (Trypsin Gold, Promega, WI, USA). The digested tryptic peptides were desalted by Zip-tip C_{18} (Millipore, MA, USA). Peptides were eluted from the Zip-tip with 0.5 μl of matrix solution (α-cyano-4-hydroxycinnamic acid (5 mg/ml in 50% acetonitrile, 0.1% trifluoroacetic acid, 25 mM ammonium bicarbonate) and spotted on the MALDI plate (model ABI 01-192-6-AB). MALDI-TOF MS and TOF/TOF tandem MS/MS were performed on an ABI 4700 mass spectrometer (Applied Biosystems, MA, USA). MALDI-TOF mass spectra were acquired in reflectron positive ion mode, averaging 4,000 laser shots per spectrum. TOF/TOF tandem MS fragmentation spectra were acquired for each protein, averaging 4,000 laser shots per fragmentation spectrum on each of the ten most abundant ions present in each sample (excluding trypsin autolytic peptides and other known background ions). Both of the resulting peptide mass and the associated fragmentation spectra were submitted to GPS Explorer workstation equipped with MASCOT search engine (Matrix science, London, UK) to search National Center for Biotechnology Information non-redundant (NCBInr). Searches were performed without constraining protein molecular weight or isoelectric point, with variable carbamidomethylation of cysteine and oxidation of methionine residues, and with one missed cleavage also allowed in the search parameters. Candidates with either protein score C.I. % or Ion C.I. % greater than 95 were considered significant.

5. Reverse Immunoprecipitation

$SAOS_2$ cells were treated with NELL-1-his 5 min. 50μl of the Protein G beads slurry (Santa Cruz #SC-2003, CA, USA, PBS pre-washed slurry) was transferred to 500 μl of cold lysis buffer. The samples were centrifused at 1,000×g for 30 seconds, and then the lysis buffer was removed for preclearance. The washed beads were washed two more times with 500 μl of cold lysis buffer, and resuspended in the same buffer. 500 μg of cell lysate was added to the prepared protein G slurry. Samples were incubated at 4°C for one hour. The samples were centrifused at 1,000×g for 1 minute at 4°C and the supernatant was transferred to fresh eppendorfs. 500 μg of cellular protein was transferred to a 1.5 ml microcentrifuge tube. 2 μg of primary antibody (Anti Vimentin Ab, Santa Cruz, CA, USA) was added and incubated for 1 hour at 4°C. For control group, no antibody was added. Samples were incubated at 4°C overnight on a shaker. The immunocomplex was washed three times with the lysis buffer. After the final wash, each pellet was resuspended in 2× sample buffer and a total of 40 μl of sample was resolved by electrophoresis and transferred to nitrocellulose and Western blot analysis was performed with HisProbe™-HRP anti-His antibodies for the detection of NELL-1-his in the immunocomplex. Washed beads without Anti-Vimentin were used as negative control.

Results

1. Far-Western analysis in $SAOS_2$, WI38, and Primary Calvarial Cells

The total membrane protein lysates were analyzed with the Far-Western blot technique using NELL-1-his as the primary ligand (Fig. 1). The cells were harvested at different time points; 2, 24 and 48 hrs after differentiation medium treatment, lanes 1~4 respectively. Interestingly, the lower band (~55 kDa) demonstrated the strongest signal with the 48 hours time point, whereas no band was visualized with the 2 hours differentiation media incubation. Two bands at approximately 75 kDa and 55 kDa were evident with the 24 and 48 hours differentiation media treatment. Human embryonic fibroblasts, WI38 showed no 55 kDa band, which is interesting because this cell line has not been shown to respond to NELL-1. The results from primary calvarial cells (data not shown) also showed two bands around the same size, especially the lower band around 55 kDa which had a stronger signal than 75 kDa band.

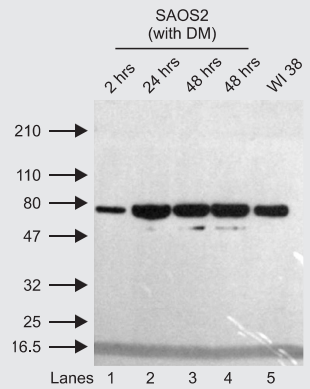

Figure 1. Far-Western blot analysis of binding proteins. Lane1: 2 hrs differentiation medium treatment, Lane 2: 24 hrs differentiation medium treatment, Lanes 3 and 4: 48 hrs differentiation medium treatment. Intensity of the lower band (~55 kDa) increased from 2 hrs to 48 hrs, Lane 5: 48 hrs differentiation medium treated to WI 38 (human embryonic fibroblast). Two bands, 75 kDa and 55 kDa were evident in 24 and 48 hours differentiation media treatment in $SAOS_2$. Human embryonic fibroblast WI38 showed no 55 kDa band at 48 hrs time point.

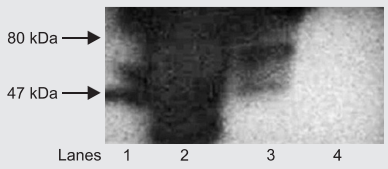

Figure 2. Immunoprecipitation followed by immunoblotting with HisProbe™-HRP anti-His antibodies. Lane1: Membrane protein, Lane2: NELL-1-His-resin complex (positive control), Lane3: Immunocomplex of extracted protein-NELL-1-his-resin (experimental IP), Lane 4: Extracted protein-resin complex (negative control).

2. Immunoprecipitaion and Far-Western

Since it is known that protein to bead interactions can be compromised by detergents, binding efficiency studies were conducted first with PBS and RIPA washing buffer to obtain optimal conditions for maximal NELL-1-his binding. Based on the results, PBS was selected as the washing buffer with about 50% efficiency; e.g. when 40 μg of NELL-1-his was used initially, approximately 20 μg would be retained. Immunoprecipitations of $SAOS_2$ and primary calvarial cells with NELL-1-his-resin followed by gel staining were compared to determine which cells had stronger binding to NELL-1. Immunoprecipitation samples were comprised of NELL-1-his-resin plus protein immunocomplex and control samples consisted of resin and protein lysis immunocomplex without NELL-1-his. NELL-1-his-resin complex was used as a positive control. Cell optimization studies showed that primary calvarial cells had greater consistency in binding than $SAOS_2$ and therefore were used in the remaining studies. Immunoprecipitation of extracted protein from primary calvarial cells with NELL-1-his-resin complex was followed by immunoblotting with HisProbe™-HRP anti-

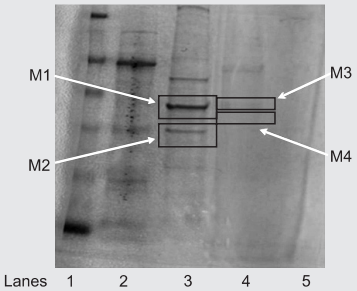

Figure 3. Immunoprecipitation of primary calvarial cells. Lane 1: Marker, Lane 2: NELL-1-his-resin complex (positive control), Lane 3: Cell lysate, Lane 4: Immunocomplex of extracted protein-NELL-1-his-resin (experimental IP), Lane 5: Extracted protein-resin complex (negative control). The red boxes indicate bands analyzed using mass spectrometry.

bodies against NELL-1-his (Fig. 2). These results demonstrated that NELL-1-his cross-reacts with certain proteins located around 75 kDa and 55 kDa. Gel staining and immunoprecipitation followed by Far-Western was performed to isolate bands for protein analysis (Fig. 3).

3. Protein identification

Distinct bands from experiments in Fig. 3. were used in one-dimensional gel electrophoresis followed by TOF/TOF tandem MS to identify candidate proteins. This technique was chosen for its capacity to identify multiple proteins present in a single protein band with high confidence so that even low-abundance proteins, if present, will be detected. M1, M2, M3, and M4 bands were labeled as shown in Fig. 3. Comparison of M1 and M3 bands revealed significant results. M1 was visualized in the protein lysate prior to immunoprecipitation, and M3 was visualized after immunoprecipitation. The only confirmative protein result from both bands was Vimentin. M2 band analysis revealed significant number of actin proteins. The M2 band, while visualized in the membrane protein lysate, was undetectable in the immunoprecipitaion sample using both gel staining assay and Far-Western analysis. No significant proteins was identified from the M4 band. The 75 kDa and 55 kDa bands from $SAOS_2$ cell lines shown in Fig. 1 were cut and the individual proteins within these bands were identified using mass spectrometry. Vimentin was among a number of other proteins also identified (Data not shown).

4. Reverse IP

$SAOS_2$ cells were treated with NELL-1-his 5 min. Immunoprecipitation samples were comprised of extracted protein-Vimentin Ab-Bead (experimental IP) and control samples consisted of bead and protein lysis immunocomplex without Vimentin Ab. Cell-lysis was used as a positive control (Fig. 4).

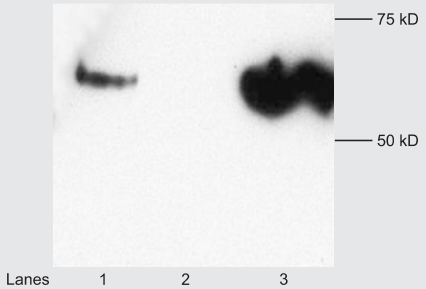

Figure 4. Immunoprecipitation followed by immunoblotting with HisProbe™-HRP anti-His antibodies to detect NELL-1-his. Lane 1: Immunocomplex of extracted protein-Vimentin Ab-Bead (experimental IP), Lane 2: Immunocomplex of extracted protein-Bead, Lane 3: Cell lysate only.

Discussion

The objective of this research is to find the potential NELL-1 binding protein associated with the membrane portion of cells, which would provide a mechanism through which NELL-1 functions. To address this question, we performed Far-Western (Figs. 1, 2), immunoprecipitations (Fig. 3), combination of both (Fig. 4) followed by mass spectroscopy to find and identify new NELL-1 binding proteins. We demonstrate here that NELL-1 can bind Vimentin, an intermediate filament.

Initially, two bands were detected with Far-Western Analysis (Fig. 1), and were analyzed using mass spectroscopy. In order to reduce the number of potential candidates proteins we optimized conditions including the type of cell and extraction buffer as well as experiemental design, immunoprecipitation with or without Far-Western analysis. Between the two cells, primary calvarial cells were selected due to consistent binding compared with $SAOS_2$. In agreement with the Far-Western band signals, approximately same-size bands reappeared. However, this combined technique was complicated by two factors. First, NELL-1-his appeared too disintegrated (Fig. 2) to serve as a positive control. To address this issue, gel staining was performed in each experiment. Secondly, the binding between NELL-1-his to TALON Metal Affinity Resin or NELL-1-his to potential binding protein seemed insufficient (Fig. 4). To rectify this issue, a binding affinity experiment was performed to figure out how much NELL-1 was able to bind after the washing procedure. Between two different washing buffers, PBS was selected with approximately 50% loss of NELL-1. Next, non-ionic and ionic RIPA buffers were tested when the cells were harvested for optimization since high efficiency protein extraction and immunocomplex protection were mutually exclusive. Visualization of the band patterns in different buffers revealed that the 55 kDa band seemed to have the greatest binding. The other 3 bands were moved to supernatant when NP40 (non-ionic detergent) was added first rather than Tris-HCl only. The remaining pellet was resuspended in ionic detergent, and eventually the 55 kDa band was the only one remaining. This signified the importance

of this band. Also, this optimization had an enhancing effect of better contrast which was facilitated following mass spectroscopy. Four bands were cut and analyzed by mass spectroscopy (TOF/TOF tandem MS, Fig. 3). The most interesting finding was the comparison between M1 and M3 which showed same size bands, the former was from protein lysate, and the latter from the immunnocomplex. Vimentin was detected in both M1 and M3 bands. Even though other proteins were also identified in these bands, the confidence interval and/or protein size were not appropriate as candidates for NELL-1 binding. Vimentin is the major structural component of the intermediate filaments in mesenchymal origin cells[5]. Vimentin is also the most ubiquitous intermediate filament protein and is present in all primitive cell types, but during differentiation it is co-expressed or replaced by other intermediate filaments[6,7].

Vimentin functions in different physiological processes such as 1) integrity of cell layers and tissues in endothelial cell junctions and/or extracellular matrix interactions[8], 2) formation and turnover of adhesive structures of Integrins, cell adhesion molecules, cytoskeletal crosslinking proteins[9-14], 3) operation and organization of kinases[13-16], 4) membrane localization of receptors and formation of a functional cell surface complex in receptors and receptor-associated proteins [17-20], 5) modulation of activity through sequestration of the transcription factor[21,22], 6) modulation of activity through sequestration of cell death-regulating factors[23,24], 7) regulation of subcellular localization[24,25], 8) activation of innate immune system cells targeting extracellular domains, and 9) DNA recombination and repair in genomic DNA. In summary, Vimentin plays a versatile role such as in structural integrity of cells and tissues, adhesion and migration, signal transduction, apoptotic pathway, immune defense, and regulation of genomic DNA. NELL-1 also has versatile functions in bone formation[26]. NELL-1 accelerates chondrocyte hypertrophy and endochondral bone formation[27]. Interestingly, NELL-1 is known to bind to protein kinase C (PKC) β1, β2, δ, and ς[28] and Vimentin is also known to bind to PKCε[13], even though the subtype of PKC in the two studies were different, as a result of different cell types used in the studies. Additionally, Vimentin was reported as a key molecule of epithelial mesenchymal transition (EMT)[26]. EMT appears as a loss of epithelial polarity accompanied by an increase of cell motility, repression of the epithelial markers E-cadherin and cytokeratins, and activation of the mesenchymal marker Vimentin[29]. The developmental role of Vimentin provides a possible explanation of why primary calvarial cells isolated from 8-day-old mice have a better response to NELL-1 binding than $SAOS_2$ since NELL-1 is also known to be involved in cranial development.

According to our results, Vimentin appears to be attached to cell membranes or vesicles which might be why ionic detergents are necessary for its extraction from cell membrane. It is known that PKC-mediated phosphorylation of Vimentin is a key process in integrin traffic throughout the cell[13]. Since NELL-1 has TSPN and VWC domains which are known to bind integrin, there is the possibility that NELL-1 may bind to integrin outside of the cell and subsequently be internalized together, and bind to Vimentin internally or, *de novo* NELL-1 may bind to Vimentin. However, the physical interaction between NELL-1 and Vimentin has not been elucidated. Nevertheless, the potential relevance of the integrin involved complex formation can be hypothesized. Even though the membrane portion was extracted using the mild frozen-defrozen technique, we could not detect any cell surface receptor protein including integrins. If the protein was indeed integrin, there is a possibility that the integrin was lost during protein extraction procedure since it has been reported that integrins can reside in detergent resistant membrane rafts[30]. Another possibility is the binding between integrin and NELL-1 was not strong enough to be detected by Far-Western through the denaturing process by the reducing detergent. The function of integrin is also very similar to NELL-1 and Vimentin in terms of control of cell cycle, life and death, cell shape, orientation and movement. However, much evidence is required to prove this hypothesis. For future experiments, reverse co-immunoprecipitation using Vimentin Ab-Protein G as a decoy to detect NELL-1 in the immunocomplex will be performed for confirmation of mechanical binding between the two. A knockout mutation of Vimentin (-/-), the intermediate filament protein characteristically expressed in cells of mesenchymal origin, results in very subtle phenotypes that are not obviously related to cell fragility. Although experiments with cultured cells have described a variety of discrete changes in cell properties that are associated with Vimentin expression or organization, there is no evidence yet that any of these properties are affected in the Vimentin (-/-) mouse, whereas mouse hemizygotes for ENU-induced recessive mutations of NELL-1 exhibit gross canial defects as well as other skeletal abnormalities[31]. The phenotype of NELL-1 knock-out mice is still under investigation. The comparison between the two will provide more insight into the relationship or possible compensatory mechanism during development. For confirmative relationship between NELL-1 and Vimentin, binding affinity assay using a

competitor, response of Vimentin knock out cell to NELL-1, and immunofluorescence for co-localization will be considered in further research endeavors. The possible integrin involvement hypothesis will be addressed cautiously beginning with integrin subtype expression assays among different cells lines, of which some are known to respond to NELL-1, and then co-immunoprecipitation studies will be performed.

Conclusion

The present study suggests a new interaction between NELL-1 and Vimentin which also seems to be functionally consistent in terms of cell differentiation, proliferation, and death.

References

1. McGillivray G, Savarirayan R, Cox TC, Stojkoski C, McNeil R, Bankier A, Bateman JF, Roscioli T, Gardner RJ, Lamandé SR. Familial scaphocephaly syndrome caused by a novel mutation in the FGFR2 tyrosine kinase domain. J Med Genet. 2005; 142: 656-62.
2. Nagase T, Nagase M, Hirose S, Ohmori K. Crouzon synodrome with acanthosis nigricans: a case report and mutational analysis. Cleft Palate Craniofac J. 2000; 137: 78-82.
3. Ting K, Vastardis H, Mulliken JB, Soo C, Tieu A, Do H, Kwong E, Bertolami CN, Kawamoto H, Kuroda S, Longaker MT. Human NELL-1 expressed in unilateral coronal synostosis. J Bone Miner Res. 1999; 14: 80-9.
4. Tompkins K, George A, Veis A. Characterization of a mouse amelogenin [A-4]/M59 cell surface receptor. Bone. 2006; 38: 172-80.
5. Franke WW, Hergt M, Grund C. Rearrangement of the vimentin cytoskeleton during adipose conversion: formation of an intermediate filament cage around lipid globules. Cell. 1987; 49: 131-41.
6. Hendrix MJ, Seftor EA, Seftor RE, Trever KT. Experimental co-expression of vimentin and keratin intermediate filaments in human breast cancer cells results in phenotypic interconversion and increased invasive behavior. Am J Pathol. 1997; 150: 483-95.
7. Dandachi N, Hauser-Kronberger C, More E, Wiesener B, Hacker GW, Dietze O, Wirl G. Co-expression of tenascin-C and vimentin in human breast cancer cells indicates phenotypic transdifferentiation during tumour progression: correlation with histopathological parameters, hormone receptors, and oncoproteins. J Pathol. 2001; 193: 181-9.
8. Nieminen M, Henttinen T, Merinen M, Marttila-Ichihara F, Eriksson JE, Jalkanen S. Vimentin function in lymphocyte adhesion and transcellular migration. Nat Cell Biol. 2006; 8: 156-62.
9. Homan SM, Mercurio AM, LaFlamme SE. Endothelial cells assemble two distinct alpha6beta4-containing vimentin-associated structures: roles for ligand binding and the beta4 cytoplasmic tail. J Cell Sci. 1998; 111: 2717-28.
10. Gonzales M, Weksler B, Tsuruta D, Goldman RD, Yoon KJ, Hopkinson SB, Flitney FW, Jones JC. Structure and function of a vimentin-associated matrix adhesion in endothelial cells. Mol Biol Cell. 2001; 12: 85-100.
11. Tsuruta D, Jones JC. The Vimentin cytoskeleton regulates focal contact size and adhesion of endothelial cells subjected to shear stress. J Cell Sci. 2003; 116: 4977-84.
12. Kreis S, Schönfeld HJ, Melchior C, Steiner B, Kieffer N. The intermediate filament protein vimentin binds specifically to a recombinant integrin alpha2/beta1 cytoplasmic tail complex and co-localizes with native alpha2/beta1 in endothelial cell focal adhesions. Exp Cell Res. 2005; 305: 110-21.
13. Ivaska J, Vuoriluoto K, Huovinen T, Izawa I, Inagaki M, Parker PJ. PKCepsilon-mediated phosphorylation of vimentin controls integrin recycling and motility. EMBO J. 2005; 24: 3834-45.
14. Correia I, Chu D, Chou YH, Goldman RD, Matsudaira P. Integrating the actin and vimentin cytoskeletons:adhesion-dependent formation of fimbrin–vimentin complexes in macrophages. J Cell Biol. 1999; 146: 831-42.
15. Sin WC, Chen XQ, Leung T, Lim L. RhoA-binding kinase alpha translocation is facilitated by the collapse of the vimentin intermediate filament network. Mol Cell Biol. 1998; 18: 6325-39.
16. Janosch P, Kieser A, Eulitz M, Lovric J, Sauer G, Reichert M, Gounari F, Büscher D, Baccarini M, Mischak H, Kolch W. The Raf-1 kinase associates with vimentin kinases and regulates the structure of vimentin filaments. FASEB J. 2000; 14: 2008-21.
17. Perlson E, Hanz S, Ben-Yaakov K, Segal-Ruder Y, Seger R, Fainzilber M. Vimentin-dependent spatial translocation of an activated MAP kinase in injured nerve. Neuron. 2005; 45: 715-26.
18. Runembert I, Queffeulou G, Federici P, Vrtovsnik F, Colucci-Guyon E, Babinet C, Briand P, Trugnan G, Friedlander G, Terzi F. Vimentin affects localization and activity of sodium–glucose cotransporter SGLT1 in membrane rafts. J Cell Sci. 2002; 115: 713-24.
19. Faigle W, Colucci-Guyon E, Louvard D, Amigorena S, Galli T. Vimentin filaments in fibroblasts are a reservoir for SNAP23, a component of the membrane fusion machinery. Mol Biol Cell. 2000; 11: 3485-94.
20. Kumar N, Robidoux J, Daniel KW, Guzman G, Floering LM, Collins S. Requirement of vimentin filament assembly for beta3-adrenergic receptor activation of ERK MAP kinase and lipolysis. J Biol Chem. 2007; 282: 9244-50.
21. Yang X, Wang J, Liu C, Grizzle WE, Yu S, Zhang S, Barnes S, Koopman WJ, Mountz JD, Kimberly RP, Zhang HG. Cleavage of p53-vimentin complex enhances tumor necrosis factor-related apoptosis-inducing ligand-mediated apoptosis of rheumatoid arthritis synovial fibroblasts. Am J Pathol. 2005; 167: 705-19.
22. Lopez-Egido J, Cunningham J, Berg M, Oberg K, Bongcam-Rudloff E, Gobl A. Menin's interaction with glial fibrillary acidic protein and

References

vimentin suggests a role for the intermediate filament network in regulating menin activity. Exp Cell Res. 2002; 278: 175-83.

23. Schietke R, Bröhl D, Wedig T, Mücke N, Herrmann H, Magin TM. Mutations in vimentin disrupt the cytoskeleton in fibroblasts and delay execution of apoptosis. Eur J Cell Biol. 2006; 85: 1-10.
24. Stefanovic S, Windsor M, Nagata KI, Inagaki M, Wileman T. Vimentin rearrangement during African swine fever virus infection involves retrograde transport along microtubules and phosphorylation of vimentin by calcium calmodulin kinase II. J Virol. 2005; 79: 11766-75.
25. Bhattacharya B, Noad RJ, Roy P. Interaction between Bluetongue virus outer capsid protein VP2 and vimentin is necessary for virus egress. Virol J. 2007; 4: 7-18.
26. Ivaska J, Pallari HM, Nevo J, Eriksson JE. Novel functions of vimentin in cell adhesion, migration, and signaling. Exp Cell Res. 2007; 313: 2050-62.
27. Cowan CM, Cheng S, Ting K, Soo C, Walder B, Wu B, Kuroda S, Zhang X. Nell-1 induced bone formation within the distracted intermaxillary suture. Bone. 2006; 38: 48-58.
28. Kuroda S, Tanizawa K. Involvement of epidermal growth factor-like domain of NELL proteins in the novel protein–protein interaction with protein kinase C, Biochem Biophys Res Commun. 1999; 256: 752-7.
29. Tolstonog GV, Shoeman RL, Traub U, Traub P. Role of the intermediate filament protein vimentin in delaying senescence and in the spontaneous immortalization of mouse embryo fibroblasts. DNA Cell Biol. 2001; 20: 509-29.
30. Andreolas C, Kalogeropoulou M, Voulgari A, Pintzas A. Fra-1 regulates vimentin during Ha-RAS-induced epithelial mesenchymal transition in human colon carcinoma cells. Int J Cancer. 2008; 122: 1745-56.
31. Desai J, Hughes L, Millsaps J, Stanford B, Kerley M, Carpenter D, Rinchik E, Culiat C. NELL-1, a gene coding for a novel PKC-binding protein is a candidate for late-gestation recessive lethal mutation at the L7R6 locus. Presented at the 16th international Mouse Genome Conference. 2002; San Antonio (TX).